

ANOMALOUS ABSORPTION IN CYCLIC C₃H RADICAL

Suresh Chandra¹ and S.A. Shinde

School of Physical Sciences, S.R.T.M. University,

Nanded 431 606, India

`sch@iuca.ernet.in`

Received _____; accepted _____

arXiv:astro-ph/0305324v1 19 May 2003

¹Visiting Associate, Inter-University Centre for Astronomy & Astrophysics, Pune 411 007,
India

ABSTRACT

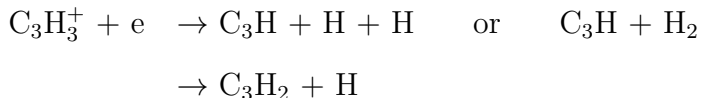
Yamamoto et al. (1987) reported the first detection of *c*-C₃H radical in TMC-1 through its transition $2_{12} \rightarrow 1_{11}$ at 91.5 GHz. Mangum and Wootten (1990) detected *c*-C₃H through the transition $1_{10} \rightarrow 1_{11}$ at 14.8 GHz in 12 additional galactic objects. The column density of *c*-C₃H in the objects was estimated to be about one order of magnitude lower than that of the C₃H₂ which is ubiquitous in the galactic objects. The most probable production mechanism of both the C₃H and C₃H₂ in dark clouds is a common dissociation reaction of C₃H₃⁺ ion (Adams & Smith, 1987). Although the *c*-C₃H is 0.8 eV less stable than its isomer *l*-C₃H, finding of comparable column densities of both the isomers in TMC-1 supports the idea of comparable formation of both the *c*-C₃H and *l*-C₃H in the cosmic objects. Existence of a metaisomer in interstellar condition is a well known phenomenon in astronomy.

We propose that *c*-C₃H may be identified through the transition $3_{31} \rightarrow 3_{30}$ at 3.4 GHz in absorption against the cosmic 2.7 K background in dense cosmic objects when no strong source is present in the background. When there is some strong source in the background of the object, peak of the absorption line decreases with the increase of the strength of the background source. However, at low densities, the intensity is found to increase. Hence, in low density regions, a background source can help in detection of the line. This absorption line may play an important role for identification of *c*-C₃H in a large number of cosmic objects. Similar absorption features are found for *c*-C₃D radical also.

Subject headings: interstellar matter - molecules - anomalous absorption

1. INTRODUCTION

Discovery of hydrocarbon ring molecules in interstellar medium has provided an important tool to investigate the medium. Cyclopropenylidene (cyclic C_3H_2 , denoted as $c-C_3H_2$) was the first hydrocarbon ring molecule discovered in astronomical objects by Thaddeus et al. (1985b). This molecule is ubiquitous in the galactic objects (Matthews and Irvine, 1985), and except in one case, its line $2_{11} \rightarrow 2_{20}$ at 21.59 GHz has always been found in absorption against the cosmic 2.7 K background (also called the cosmic microwave background, denoted as CMB) (Madden et al., 1989; Chandra & Kegel, 2001). Cox et al. (1987), however, reported this line in emission in the Planetary Nebula NGC 7027. The second hydrocarbon ring molecule, cyclopropynylidyne (cyclic C_3H , denoted as $c-C_3H$) was first detected by Yamamoto et al. (1987) in TMC-1 through its transition $2_{12} \rightarrow 1_{11}$ at 91.5 GHz. Mangum and Wootten (1990) detected $c-C_3H$ through the transition $1_{10} \rightarrow 1_{11}$ in 12 additional galactic objects. The $l-C_3H$ (linear C_3H) also has been identified in astronomical objects (Thaddeus et al., 1985a). The most probable production mechanism of C_3H and C_3H_2 in dark clouds is a common dissociation reaction of $C_3H_3^+$ ion (Adams & Smith, 1987):



Although $c-C_3H$ is 0.8 eV less stable than $l-C_3H$, the column density of $c-C_3H$ is found almost comparable to that of $l-C_3H$ in TMC-1. Such a metastable isomer can exist in the interstellar condition. For example, the HNC, the isomer of HCN, is detected in various molecular clouds. In the preset *Letter*, we propose to identify $c-C_3H$ in cosmic objects through $3_{31} \rightarrow 3_{30}$ transition in absorption against the CMB.

2. MOLECULAR DATA & CALCULATIONS

The c -C₃H is an a -type asymmetric top molecule with electric dipole moment $\mu = 2.4$ Debye. Rotational levels in an asymmetric top molecule are specified as J_{k_a, k_c} , where J is the rotational quantum number, and k_a and k_c the projections of J on the axis of symmetry in case of prolate and oblate symmetric tops, respectively. In a -type asymmetric top molecule, rotational radiative transitions are governed by the selection rules:

$$\begin{aligned}
 J : & \quad \Delta J = 0 \pm 1 \\
 k_a, k_c : & \quad \text{even, odd} \longleftrightarrow \text{even, even} \\
 & \quad \text{odd, even} \longleftrightarrow \text{odd, odd}
 \end{aligned}$$

Owing to the nuclear symmetry in c -C₃H, rotational levels with even value of k_a are missing in its spectra. As the temperature in dark molecular clouds is not large, in the present investigation we accounted for the rotational levels up to 77 cm^{-1} for c -C₃H (Table 1). The Einstein A -coefficient for rotational transitions between the levels are calculated following the method discussed by Chandra & Sahu (1993) and Chandra & Rashmi (1998). These 37 rotational levels are connected through 121 radiative transitions. For the calculations, the required molecular and distortional constants are taken from Yamamoto and Saito (1994). We have not, however, accounted for fine structure and hyperfine structure splittings of the levels.

NLTE occupation numbers of energy levels are calculated in an *on-the-spot* approximation discussed by Rausch et al. (1996), where the external radiation field, impinging on a volume element generating the lines, is the CMB only. Besides the radiative transition probabilities for radiatively allowed transitions between the rotational levels, data required for the present investigation are the rate coefficients for collisional transitions between the levels due to collisions with H₂ molecules. Collisional rate coefficients are not available in literature. Therefore, the rate coefficients for downward transitions

$J'_{k_a k'_c} \rightarrow J_{k_a k_c}$ at a kinetic temperature T are taken as (Sharma & Chandra, 2001)

$$C(J'_{k_a k'_c} \rightarrow J_{k_a k_c}) = 1 \times 10^{-11} \sqrt{T/30} / (2J' + 1)$$

For upward collisional rate coefficients, we accounted for the fact that downward and upward collisional rate coefficients are related through the detailed equilibrium (Chandra & Kegel, 2000).

3. RESULTS & DISCUSSION

In order to include a large number of cosmic objects where c -C₃H may be found, numerical calculations are carried out for wide ranges of physical parameters. The molecular hydrogen density n_{H_2} has been varied over the range from 10^3 cm^{-3} to 10^7 cm^{-3} , and calculations are performed for three kinetic temperatures 10, 20 and 30 K. In the calculations, free parameters are the molecular hydrogen density n_{H_2} , and $\gamma \equiv n_{mol}/(dv_r/dr)$, where n_{mol} is density of the c -C₃H molecule, and dv_r/dr the velocity gradient. As we have used scaled values of collisional rates, our results are qualitative in nature.

3.1. ANOMALOUS ABSORPTION IN c -C₃H RADICAL

Out of a number of lines of c -C₃H found in absorption against the CMB, the transition $3_{31} \rightarrow 3_{30}$ at 3.4 GHz has shown reasonably good absorption phenomenon. The Einstein A -coefficient for this line is $1.9 \times 10^{-9} \text{ s}^{-1}$, and the radiative lifetimes of the upper and lower levels 3_{30} and 3_{31} are $2.3 \times 10^4 \text{ s}$ and $4.4 \times 10^4 \text{ s}$, respectively. Observation of a spectral line in absorption against the CMB is an unusual phenomenon. The intensity, I_ν , of a line

generated in an interstellar cloud, with homogeneous excitation conditions, is given by

$$I_\nu - I_{\nu,bg} = (S_\nu - I_{\nu,bg})(1 - e^{-\tau_\nu})$$

where $I_{\nu,bg}$ is the intensity of the continuum against which the line is observed, τ_ν the optical depth of the line, and S_ν the source function. For positive optical depth, observation of an interstellar line in absorption against the CMB, obviously, implies the excitation temperature of the line, T_{ex} , to be less than the CMB temperature 2.7 K, but positive. It requires rather peculiar conditions in the molecule generating the line.

Variation of line-intensity against the CMB in the units of the Planck's function at the kinetic temperature of $T(K)$, i.e., $(I_\nu - I_{\nu,bg})/B_\nu(T)$, for the line $3_{31} \rightarrow 3_{30}$ for three kinetic temperatures 10, 20 and 30 K (written on the top of the column) is shown in Figure 1 (first row) for $\gamma = 10^{-6}$ and $10^{-5} \text{ cm}^{-3} (\text{km/s})^{-1} \text{ pc}$. The line $3_{31} \rightarrow 3_{30}$ shows the absorption against the CMB. The excitation temperature of the line reduces up to 0.27 K which 10% of the CMB temperature, and its absorption intensity is comparable to the absorption intensity of the line $2_{11} \rightarrow 2_{20}$ of $c\text{-C}_3\text{H}_2$ calculated by Chandra & Kegel (2001). It supports the idea of detection of the line $3_{31} \rightarrow 3_{30}$ of $c\text{-C}_3\text{H}$ in absorption against the CMB.

3.2. EFFECT OF A BACKGROUND SOURCE

In the above discussion, we considered the external radiation field, impinging on a volume element generating the lines, to be the CMB only. In order to see the effect of a background source, we repeated the calculations for the background intensity

$$I_{\nu,bg} = (1 - f)B_\nu(2.7K) + fB_\nu(2000K)$$

f is the dilution factor, representing the distance of the background source from the cosmic object, and the effect of the atmosphere between the source and the object. Here, the

temperature of the background source is assumed to be 2000 K. For other values of the temperature of the source, the effect can be scaled down with the help of the dilution factor f . The case $f = 0$ corresponds to the CMB only. With the increase of the value of f the peak of the absorption line decreases. However, at low densities, the intensity increases. Hence, in the low density regions, a background source can help in detection of the line. Figure 1 shows the absorption intensities for $f = 0, 10^{-4}$ and 10^{-3} . When f is large than 10^{-3} , the absorption feature disappears.

3.3. ANOMALOUS ABSORPTION IN c -C₃D RADICAL

We repeated the calculations for c -C₃D radical, where we accounted for the rotational levels given in Table 1. Note that the sequence of some higher levels of c -C₃D is changed relative to those of the c -C₃H. This molecule also is an a -type asymmetric top molecule with electric dipole moment $\mu = 2.4$ Debye. The required molecular and distortional constants are taken from Yamamoto and Saito (1994). Here, also the line $3_{31} \rightarrow 3_{30}$ at 0.9 GHz is found in absorption against the CMB. Variation of line-intensity against the CMB in the units of Planck's function at the kinetic temperature of T (K), i.e., $(I_\nu - I_{\nu,bg})/B_\nu(T)$, for the line for three kinetic temperatures 10, 20 and 30 K and the dilution factor $f = 0, 10^{-4}$ and 10^{-3} is shown in Figure 2 for $\gamma = 10^{-6}$ and $10^{-5} \text{ cm}^{-3} (\text{km/s})^{-1} \text{ pc}$. The line $3_{31} \rightarrow 3_{30}$ of c -C₃D is found to be weaker than that of the c -C₃DH. However, the features of the two are very similar.

We re grateful to Prof. J.V. Narlikar, Prof. S.A. Suryawanshi, and Prof. Dr. W.H. Kegel for encouragement.

REFERENCES

- Adams, N.G. & Smith, D. 1987, *ApJ***317**, L25
- Chandra, S. & Kegel, W.H., 2000 *A&AS***142**, 113
- Chandra, S. & Kegel, W.H., 2001 *A&A*, **367**, 995
- Chandra, S. & Rashmi, 1998 *A&AS***131**, 137
- Chandra, S. & Sahu, A., 1993 *A&A***272**, 700
- Cox, P., Güsten, R. & Henkel, C. 1987 *A&A*, **181**, L19
- Madden, S.C., Irvine, W.M., Matthews, H.E., Friberg, P. & Swade, D.A. 1989, *AJ*, **97**, 1403
- Mangum, J.G. & Wootten, A. 1990, *A&A*, **239**, 319
- Matthews, H.E. & Irvine, W.M. 1985, *ApJ***298**, L61
- Rausch, E., Kegel, W.H., Tsuji, T. & Piehler, G., 1996, *A&A***315**, 533
- Sharma, A.K. & Chandra, S., 2001, *A&A*, **376**, 333
- Thaddeus, P., Gottlieb, C.A., Hjalmarson, A., Johansson, L.E.B., Irvine, W.M., Friberg, P.
& Linke, R.A. 1985a, *ApJ*, **294**, L49
- Thaddeus, P., Vrtilik, J.M. & Gottlieb, C.A. 1985b, *ApJ*, **299**, L63
- Yamamoto, S. & Saito, S. 1994, *J. Chem. Phys.*, **101**, 5484
- Yamamoto, S., Saito, S. & Murakami, A. 1987, *ApJ*, **322**, L55

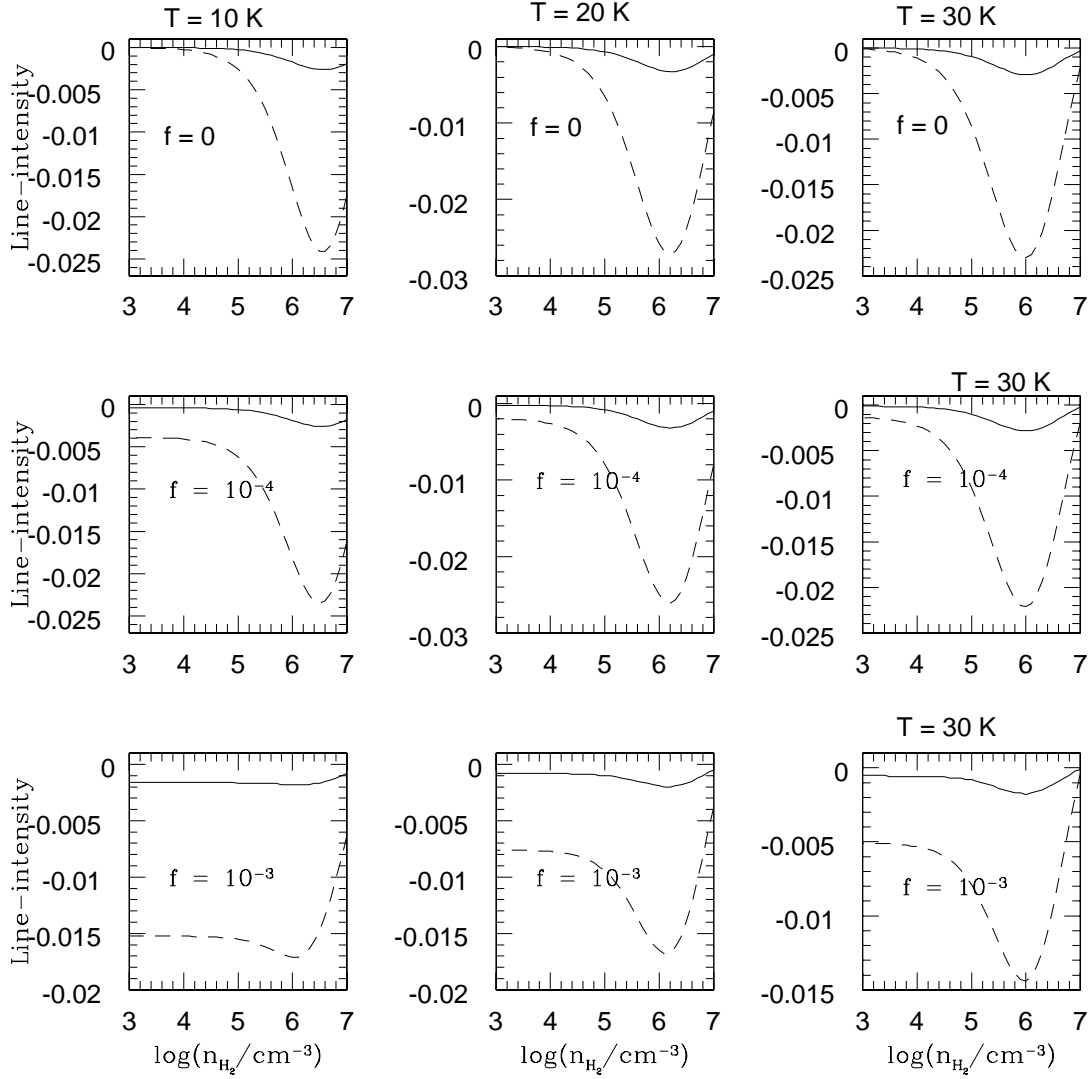


Fig. 1.— Variation of line-intensity against the CMB in the units of Planck’s function at the kinetic temperature of $T(\text{K})$, i.e., $(I_\nu - I_{\nu,bg})/B_\nu(T)$, for the transition $3_{31} \rightarrow 3_{30}$ of $c\text{-C}_3\text{H}$ radical for three kinetic temperatures 10 20, and 30 K (written at the top of each column) with dilution factor f written there. Negative value of line-intensity shows absorption against the CMB. Solid line is for $\gamma = 10^{-6} \text{ cm}^{-3} (\text{km/s})^{-1} \text{ pc}$ and dotted line for $\gamma = 10^{-5} \text{ cm}^{-3} (\text{km/s})^{-1} \text{ pc}$

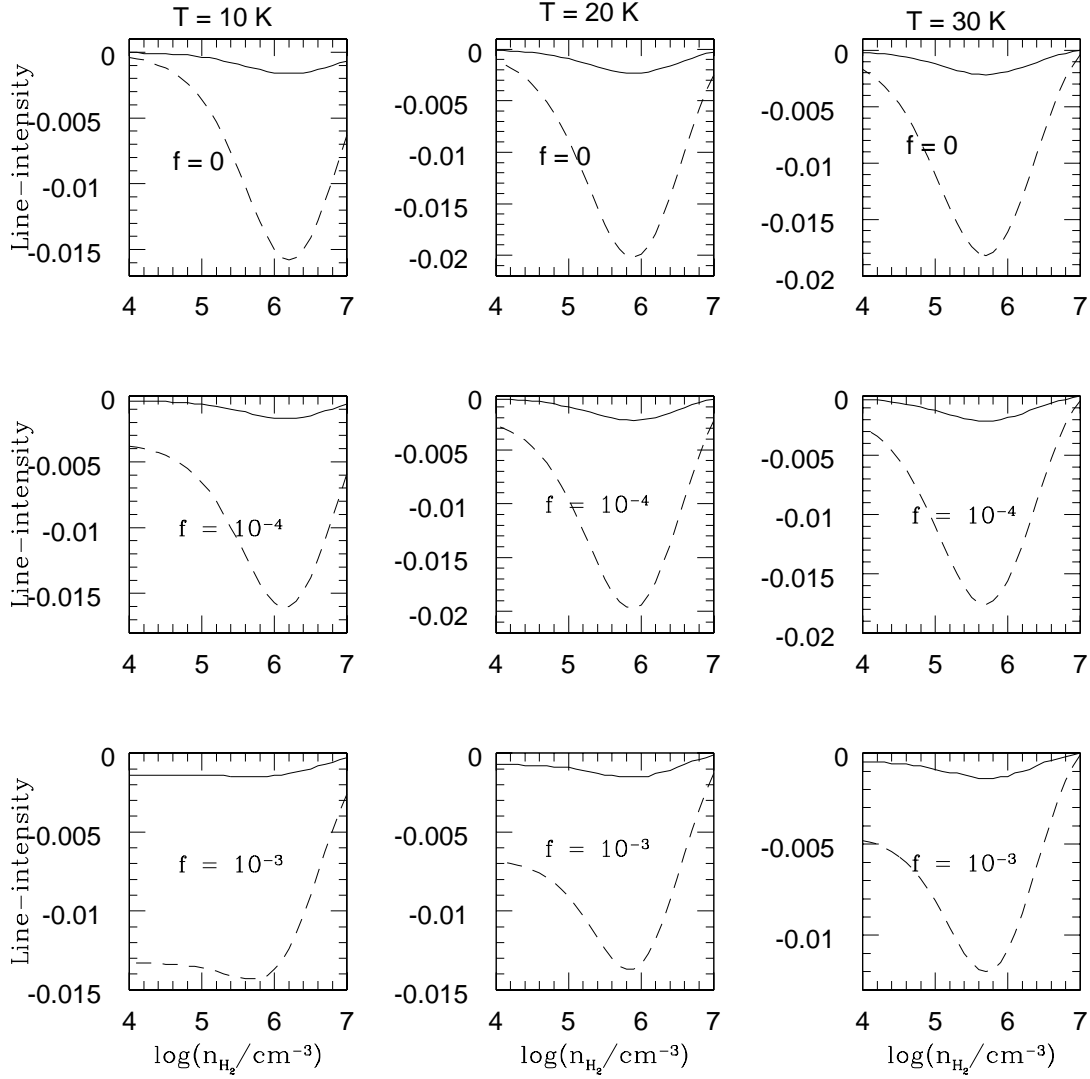


Fig. 2.— Variation of line-intensity against the CMB in the units of Planck’s function at the kinetic temperature of $T(\text{K})$, i.e., $(I_\nu - I_{\nu,bg})/B_\nu(T)$, for the transition $3_{31} \rightarrow 3_{30}$ of $c\text{-C}_3\text{D}$ radical for three kinetic temperatures 10 20 and 30 K (written at the top of each column) with dilution factor f written there. Negative value of line-intensity shows absorption against the CMB. Solid line is for $\gamma = 10^{-6} \text{ cm}^{-3} (\text{km/s})^{-1} \text{ pc}$ and dotted line for $\gamma = 10^{-5} \text{ cm}^{-3} (\text{km/s})^{-1} \text{ pc}$

Table 1. Rotational energy levels of *c*-C₃H & *c*-C₃D radicals

<i>J</i>	<i>k_a</i>	<i>k_c</i>	<i>E</i> (cm ⁻¹)		<i>J</i>	<i>k_a</i>	<i>k_c</i>	<i>E</i> (cm ⁻¹)	
			<i>c</i> -C ₃ H	<i>c</i> -C ₃ D				<i>c</i> -C ₃ H	<i>c</i> -C ₃ D
1	1	1	2.126	2.055	5	5	1	41.864	40.995
1	1	0	2.620	2.416	5	5	0	41.876	40.996
2	1	2	5.180	4.695	6	3	4	43.515	38.776
2	1	1	6.664	5.779	6	3	3	46.751	40.312
3	1	3	9.620	8.586	7	1	6	48.690	43.154
3	1	2	12.472	10.724	8	1	8	51.243	45.588
4	1	4	15.376	13.678	6	5	2	53.262	50.327
3	3	1	16.174	15.684	6	5	1	53.378	50.338
3	3	0	16.289	15.715	7	3	5	55.653	49.337
4	1	3	19.696	17.096	7	3	4	60.619	52.134
5	1	5	22.421	19.936	8	1	7	60.874	54.025
4	3	2	23.625	21.876	9	1	9	63.410	56.420
4	3	1	24.249	22.071	7	5	3	66.637	61.287
5	1	4	28.128	24.694	7	5	2	67.177	61.348
6	1	6	30.748	27.345	8	3	6	69.120	61.194
5	3	3	32.792	29.594	9	1	8	74.336	66.020
5	3	2	34.490	30.256	8	3	5	75.712	65.522
6	1	5	37.780	33.385	10	1	10	76.856	68.391
7	1	7	40.356	35.896					